CHAPTER 3

MODEL APPLICABILITY

3.1. DATA COLLECTION

3.1.1. Field trip overview

High-quality in situ measurements are prerequisite for satellite data product validation, algorithm development, and many environment-related problems. Initial as well as follow-up field validation is necessary to ensure regular calibration of remote sensing algorithms and thus continuous accuracy of the final product. This section provides an overview of fieldwork carried out in the Lucinda region in 2002-2004 in association with the present study.

In the course of the present work four field trips were conducted in the coastal and estuarine waters adjacent to the Herbert River, covering two dry seasons (10-14 July 2002, 21-22 October 2003) and two wet seasons, the first characterised by low Herbert river discharge (19-24 February 2003) and the second covering a moderate flood (8-21 February 2004). The two February expeditions were carried out in cooperation with a research group from James Cook University (group leader Prof. Mal Heron, Mal.Heron@jcu.edu.au). The list of projects and their participants for the February 2004 field trip can be found in Appendix 3.

Three types of data were collected during the field trips, and the summary of measurements carried out in the Lucinda region is presented in Table 3.1. The first type of date supported direct comparison between measured in situ and satellite-derived biogeochemical quantities, with the ultimate goal of validating the bio-optical algorithm developed in the present work. Measured biogeochemical parameters in this group included chlorophyll concentration, total suspended sediment concentration, and coloured dissolved organic matter absorption spectra, all measured in surface waters. Throughout the present work these quantities are referred to as "in situ measurements", although strictly speaking they are all in vitro (i.e. outside the natural environment) measurements. Environmental surveying accompanied water sampling at each station and included the following data: GPS location, cloud cover, sea state, wind speed, sea surface temperature and salinity, water depth, visibility, turbidity and colour (in situ photography).

The second type of data comprised of the same set of parameters as the first group but measured outside the temporal and spatial ranges of SeaWiFS and MERIS overpasses. Measurements were carried out (i) on direct SeaWiFS overpass days before and after direct validation sampling, (ii) at various depths, and (iii) on days with no direct SeaWiFS overpass. The purposes of these measurements were (a) to gain insight into the spatial variability of water-colouring constituents and horizontal homogeneity scales in the area; (b) to assess intra-

seasonal (i.e. within season) as well as inter-seasonal (i.e. between seasons) variability in water properties; (c) to get a better understanding of the optical type of waters at Lucinda; and (d) to evaluate the vertical homogeneity of major optically significant substances in the water column.

Finally, a number of sediment-related measurements were undertaken to study flood-induced suspended sediment transport in the Herbert River and adjacent coastal waters (Chapter 4). The data collected included vertical profiles of turbidity, particle size distribution (PSD) of surface suspensions, fraction of organic matter in TSS, particulate and dissolved phosphorus concentrations, and bottom sediment density.

Measurement statistics, number	July 2002	February 2003	October 2003	February 2004	Total
Sampling days	5	6	2	14	**27**
Stations	25	21	10	107	**163**
Surface CHL concentration	86	42	10	92	**230**
CHL concentration at various depths	24	13		92	**129**
Surface CDOM absorption	16	21	10	39	**86**
CDOM absorption at various depths	17				**17**
Nutrients				27	**27**
Surface TSS concentration	14	6	10	154	**184**
Organic fraction of TSS		6	10	90	**106**
PSD		6	12	4	**22**
Sediment grab			5	18	**23**
Secchi disk depth	25	21		107	**153**
Turbidity vertical profiles				121	**121**
SeaWiFS, days	1	1	1	2	**5**
MERIS, days			1	2	**3**
Aerial photography, days			1	4	**5**

Table 3.1. Measurement statistics for 2002-2004 field expeditions at Lucinda.

3.1.2. Methodology

Water sampling

Surface water samples were collected in one-litre pre-cleaned dark plastic bottles. Depth water samples were collected with Niskin bottles. (The Niskin bottle is initially open at both ends and can be closed at the desired depth with a messenger weight, which triggers a mechanism that closes it.) The amount of seawater collected was based upon the visibility measurements (i.e. Secchi disk depths) as an approximation of light attenuation estimates. The samples were stored in foam boxes filled with ice until subsequent filtration on land.

Chlorophyll concentration

The Australian Centre for Tropical and Freshwater Research (James Cook University) carried out chlorophyll measurements. Chlorophyll and phaeophytin concentrations were determined spectrophotometrically from 90 % acetone extracts of the particulate material remaining after filtration through Whatman GF/B filters with approximately 1.0 µm pore size. APHA (1998) recommends that a nominal size for filter membranes for chlorophyll determination is 1 µm, with glass fibres preferred for filtering algae from water samples. Glass fibre membranes assist in breaking the cells when grinding, allow larger volumes of water to be filtered and do not produce a precipitate after acidification. The sample volumes varied from 250 mL to 4-5 L depending on the amount of suspended material in the sample. The filters and a 10 mL volume of 90 % acetone were added to a 50 mL pyrex tube and immediately ground for 30 seconds using a teflon pestle attached to an Analite high-speed grinder. The liquefied pulp was then immediately added to small polyethylene centrifuge tubes and refrigerated for 24 hours. After 24 hours the liquefied pulp was centrifuged at 3000 rpm for 10 min and the supernatant read in a Philips PU8620 UV-Visible spectrophotometer at 750 (background correction), 665, 664, 647 and 630 nm. After reading, 1 drop of 0.1N HCl was added to the cuvette, which was inverted and allowed to stand for 1 minute and then re-read at the same absorbance wavelengths. The following formulas were used to calculate chlorophyll and phaeophytin concentrations:

$$Chlorophyll\_a = (26.7 * (OD664_b - OD665_a) * V_e) / V_s; \quad (3.1)$$

$$Phaeophytin = (26.7 * [(1.7 * OD665_a) - OD664_b] * V_e) / V_s; \quad (3.2)$$

$$Chlorophyll\_b = 21.03 * (OD647) - 5.43 * (OD664) - 2.66 * (OD630); \quad (3.3)$$

$$Chlorophyll\_c = 24.52 * (OD630) - 7.60 * (OD647) - 1.67 * (OD664). \quad (3.4)$$

In the above formulas V_e is volume of an extract, V_s is volume of a sample, *OD* is optical density, and $OD664_a$ and $OD665_b$ are optical densities of 90 % acetone extract before and after acidification, respectively. The lowest measurable concentration was constrained by the detection limit of the spectrophotometer (0.267 mg/m^3 for 1 L of filtered water). The constant value of 0.15 mg/m^3 was adopted for such cases, but it should be kept in mind that actual concentration could be anything between 0 and 0.27 mg/m^3.

In February 2004 a Wet Labs ECO Chlorophyll Fluorometer (http://www.wetlabs.com/Products/eco/flall.htm) attached to a CTD was employed to obtain vertical profiles of chlorophyll. Concurrent with fluorometer measurements, 16 surface water

samples were collected and analysed spectrophotometrically in order to calibrate the fluorometer (Figure 3.1).

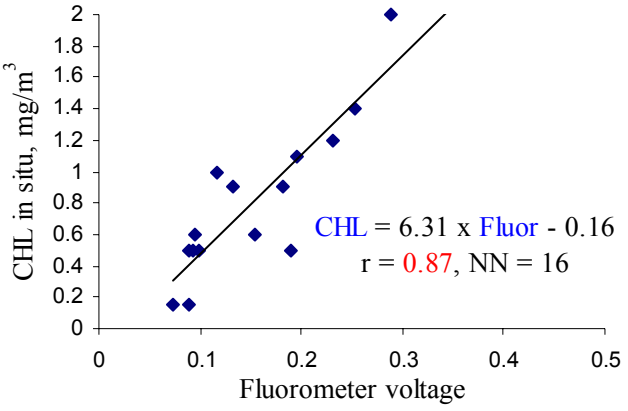

Figure 3.1. Fluorometer calibration curve

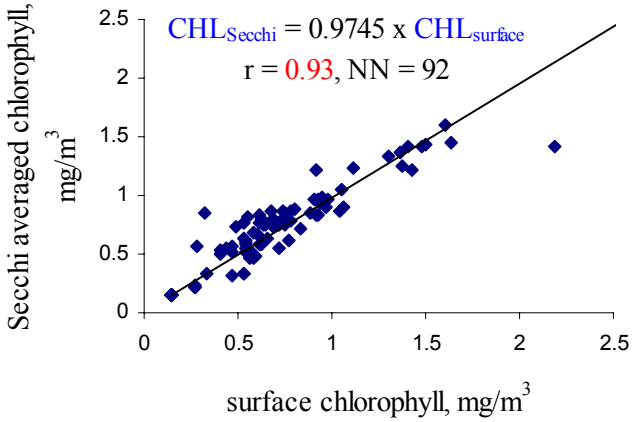

Figure 3.2. Comparison between surface and Secchi depth-averaged chlorophyll concentrations

In his pioneering paper, Gordon (1978) stated that water-leaving radiance contains signals of optically significant components averaged over the light penetration depth. In the case of vertical inhomogeneous waters, stratification has to be taken into account (Tassan 1997; Ouillon 2003). To assess the significance of this phenomenon in Lucinda waters, surface and Secchi depth-averaged chlorophyll concentrations were compared for available fluorometric vertical profiles from February 2004 and depth measurements from July 2002 and February 2003 field expeditions (Figure 3.2). Secchi depth is employed here as a crude approximation of the euphotic zone lower limit, a layer within which the downwelling irradiance falls to 1 % of the subsurface value (Kirk 1994). Due to the strong relationship found between surface and depth-averaged values, with the slope close to unity, it can be concluded that in the studied waters the subsurface chlorophyll maximum is not pronounced, i.e. the waters are vertically homogeneous. Therefore, surface concentrations can be adopted as proxies for euphotic zone averages, and in the remainder of the thesis only surface chlorophyll concentrations are considered.

Coloured dissolved organic matter absorption

Coloured dissolved organic matter (CDOM) is defined as the fraction of optically significant organic material in water which passes through a 0.22 μm MF-Millipore MCE (Mixed Cellulose Ester) membrane filter. After filtering into pre-washed and pre-combusted glass containers, samples were immediately analysed or, alternatively, stored at 4ºC in the dark

until analysis, which was carried out no later than 24 hours after filtration. Careful attention was paid to minimising contamination of water samples by organic materials and protecting them from light and possible photobleaching.

Most of the samples were analysed using a Cary 4E UV-Visible spectrophotometer and 5 cm quartz cuvettes (Gray et al 1991). The spectral absorption of CDOM a_{CDOM} was calculated using the relation:

$$a_{CDOM}(\lambda) = 2.303\, A(\lambda) / r, \qquad (3.5)$$

where $A(\lambda)$ is the absorbance or optical density measured across the cuvette pathlength, r. To account for possible contamination of particles smaller than 0.22 μm and assuming the backscatter of these particles is spectrally neutral (Green et al 1994; Babin et al 2003), a correction was applied to each measured spectrum by subtracting the absorbance value averaged over 650-700 nm from the remaining spectral values. This method as opposed to wavelength-dependent correction (Bricaud et al 1981) results in slightly lower absorption values (circa 5 % in the UV) and slightly steeper slopes for the absorption spectrum versus wavelength (Nelson et al 1998).

The absorption spectra were then fitted to the exponential equation (2.15) and CDOM absorptions at 440 nm as well as exponential slopes were derived for each of the samples. Due to photometric noise inherent in the instrument, the CDOM absorption at 440 nm was calculated as the average for 338-442 nm.

A large number of measured absorbances in the 570-700 nm region fell below the photometric reproducibility (0.0004 Abs) of the Cary 4E UV-Visible spectrophotometer (Figure 3.3). Therefore values in the 550-700 nm domain were truncated and the data were fitted to an exponential form in 400-500 nm as well as 400-550 nm domains using linear least square regression of the log-transformed

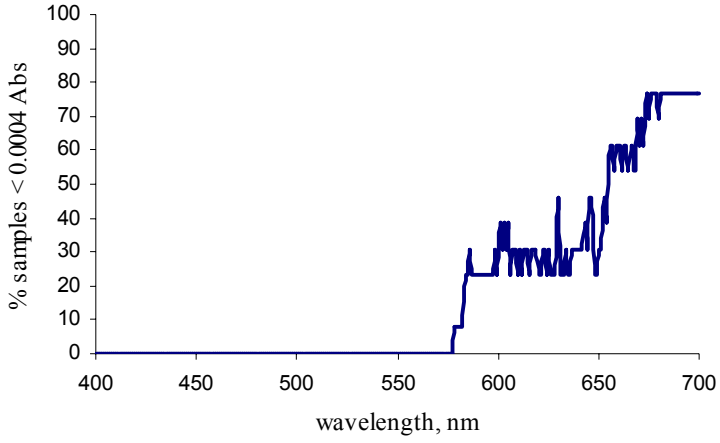

Figure 3.3. Percentage of samples with absorbances less than photometric reproducibility of the spectrophotometer 0.0004 Abs

absorption data. A goodness-of-fit statistics, R^2, was used to assess whether a simple exponential model provided a sufficient description of the data or whether it required the use of a more complicated model such as the sum of two exponentials (Kopelevich et al 1989). For Lucinda samples, R^2 was on average greater than 0.94, thus justifying the use of a one-exponent model.

Slopes calculated in the 400-550 nm range were systematically higher than those estimated in the 400-500 nm region (Figure 3.4). This is in agreement with the observational data of Kopelevich, Lutsarev et al. (1989) who related this phenomenon to fulvic and humic acids affecting various parts of the visible spectra thus resulting in different slopes.

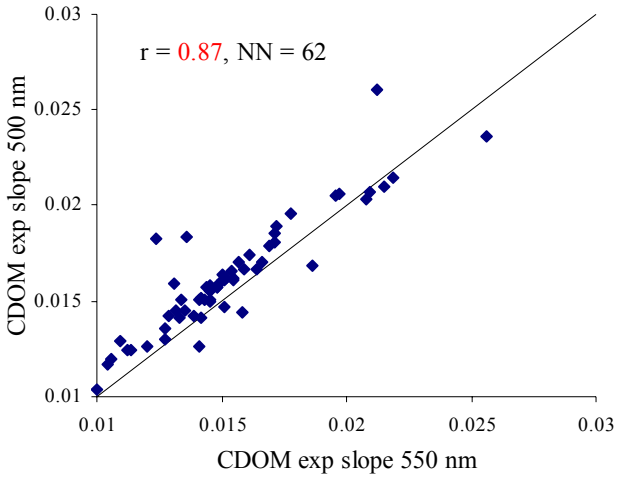

Figure 3.4. CDOM exponential slopes calculated in 400-500 nm and 400-550 nm regions

During the October 2003 field experiment five yellow substance absorption determinations were performed within 24 hours of collection using a Cary 5 UV-Visible spectrophotometer and 1 cm cuvettes. Duplicate samples were then stored in the dark for another 24 hours at 4ºC in pre-washed, pre-combusted glass containers and subsequently analysed using the Cary 4E UV-Visible spectrophotometer and 5 cm cuvettes. The difference in reference absorption $a_{CDOM}(440)$ between duplicates varied from 0 to 9 % with an average of 4.2 %. Thus storing samples at 4ºC for 24 hours did not affect measurements significantly.

Total suspended sediment concentration

Total suspended sediment concentration TSS is defined as the dry weight of the material collected on a 0.7 µm filter by seawater. The determination technique is called gravimetric filter analysis for total suspended matter, and the actual procedure is carried out in the following manner. A volume of seawater is filtered through pre-washed and pre-weighted 0.7 um glass fibre filters (Whatman GF/F filters). Normally, filtration is stopped when the filter clogs because sufficient material is then on the filter. After seawater filtration the filters are washed with 250 mL distilled water to dissolve salts, dried in an oven at 65ºC for 24 hours, cooled down to room temperature in a dessicator to avoid the uptake of atmospheric moisture, and finally weighed on an electrobalance. The concentration of TSS is calculated from the dry weight difference of filters before and after filtration divided by the sample volume and is

expressed as mg/L or equivalently g/m^3. A blank filter is used to calculate the handling error of the measurement procedure.

In February 2004, multiple TSS replicates were taken to quantify within-sample variability as well as to assess the accuracy of the gravimetric filter analysis method for deriving TSS concentrations. The average difference between replicates was 18 % and can be attributed to handling errors and limitations in the volume of water filtered due to clogging and electrobalance resolution (10^{-3} g). Contamination and loss of particles through settling or adherence to the walls of the sampler is a possible cause of variability between duplicates, which is especially true for large TSS concentrations. Also for high concentrations the accuracy of analysis decreases because a smaller amount is filtered through. Therefore, there is an optimal range of TSS that can confidently be measured using the gravimetric filter analysis method.

In February 2004 TSS concentrations were measured using four different filter pore sizes at four stations: 0.22 µm MF-Millipore MCE (Mixed Cellulose Ester) membrane filters, 0.7 µm GF/F, 8 µm Grade 40 and 20-25 µm Grade 41 filter papers. Results are presented in Figure 3.5. Glass fibre and paper filters produced an expected pattern of decreasing concentration with increasing pore size. The Millipore membrane filters (0.22 µm) results, on the other hand, were counterintuitive, with TSS < 0.22 µm sometimes less than TSS < 0.7 µm. This is due to the filter material of Millipore filters (mixed cellulose ester), which might require modification in measurement procedures. Nevertheless, TSS concentrations measured using 0.22 µm filters were related to corresponding TSS_GF/F quantities with the correlation coefficient of 0.88 (NN = 14), a statistically significant result at probability level < 0.001. The slope equals 0.87, the intercept 0.8. Using this relationship, 0.22 µm concentrations were recalculated into TSS_GF/F values for corresponding measurements during the February 2004 expedition.

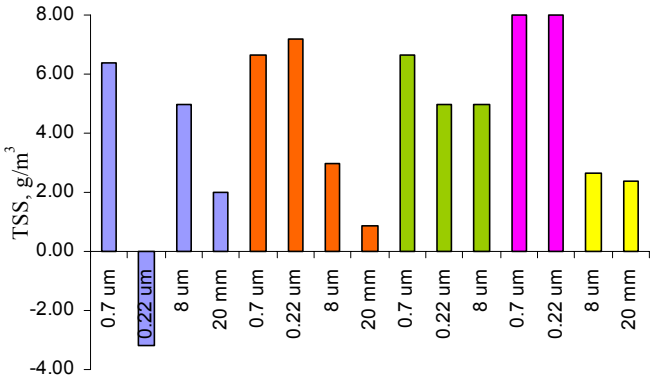

Figure 3.5. TSS measured using filters with different pore sizes. Each colour represents a station, um stands for µm.

Organic and inorganic fraction of TSS

Total suspended sediment concentration was differentiated into organic (OSS) and inorganic (ISS) fractions by burning TSS filters in a furnace at a temperature of 450ºC for 4 hours. They were then placed in a dessicator to bring them down to room temperature before weighing. The volatile fraction of TSS is presumably burnt off and loss of weight is approximately equivalent to the organic component of TSS. The material remaining on the filter is equivalent to the proportion of inorganic material in the sample.

Particle size distribution

A number of samples were analysed for particle size distribution (PSD) of surface suspended sediment matter during the field expeditions (Table 3.1). The instrument employed was a Malvern Mastersizer X Laser Diffractometer, which is based on the notion that diffraction angle is inversely proportional to particle size. A laser beam is directed into the sample volume, where particles in suspension will scatter, absorb, and reflect the beam. Scattered laser light is then received by a multielement photodetector consisting of a series of ring-shaped detectors of progressive diameters that allow measurement of the scattering angle of the beam. Particle size can be calculated from the knowledge of this angle, using full Mie theory (Rawle 1999). To avoid biodegradation of samples, an effort was made to ensure that actual analyses were performed within 24 hours of collection.

Four optical lenses were employed for PSD analyses: 45 mm (0.1-80 μm), 100 mm (0.5-180 μm), 300 mm (1.2-600 μm) and 1000 mm (4-2000 μm). This was implemented because no single lens seemed to reflect the wide range of sizes present in the water. Refractive indices used were 1.5029 for the real and 0.003 for the complex parts. The complex part of the refractive index was derived from literature sources (Stramski et al 2001; Twardowski et al 2001; Green et al 2003), while the real part was calculated according to the following considerations. Incorporating organic matter content of TSS typical for Lucinda coastal waters (0.25) and refractive indices of inorganic and organic parts of TSS (1.16 and 1.05, respectively), the refractive index relative to water was obtained as

$$\{1.17 \times (1 - 0.25) + 1.05 \times 0.25\}/1.33 = 1.5029. \quad (3.6)$$

In October 2003 and February 2004 samples at the Herbert River mouth were analysed with a number of lenses (100 mm, 300 mm and 1000 mm in October; and 45 mm and 1000 mm in February) to evaluate the consistency of results derived by using various lenses (Appendix 4,

Figure A12). The resultant distributions are similar, with slightly mismatched peak grain sizes for different optical lenses. This must be the result of the nonlinear grain-size scale used in the machine's algorithm. Peaks in the larger grain size part of the spectrum most probably represent contribution of flocs or organic matter, as those tend to have lower densities and are thus more likely to be in suspension.

Large tails at the upper end of the size ranges most probably represent machine-induced artefacts (Orpin et al 1999, Alan Orpin, e-mail communication). While indicating the presence of size fractions outside the lens limits, the magnitude of these peaks tends to be overestimated. Overall, usage of different lenses produced consistent results although caution should be exercised when interpreting extremes of the size range. The accuracy of peak grain size determination is about 5 μm for the 5-15 μm region, worsening towards coarser particles.

Junge distribution

Particle size distribution in ocean waters is often modelled by the so-called Junge hyperbolic law (Stramski et al 1991; Eisma 1993; Ulloa et al 1994; Stramski et al 2001; Twardowski et al 2001):

$$NN = k_{TSS} D^{-\beta}; \tag{3.7}$$

$$k_{TSS} = \frac{TSS}{\rho} \Big/ \frac{4}{3}\pi\left(\frac{D}{2}\right)^3, \tag{3.8}$$

where NN is the cumulative number of spherical particles with diameter greater than particle diameter D, k_{TSS} is a coefficient related to the total concentration of suspended matter (i.e. volume occupied by spherical particles each having $4/3\pi * radius^3$ volume is the mass of particles (TSS concentration) divided by their average density), β is the slope of the distribution, and ρ is the density of particles (= 2.65 g/m^3). For open ocean suspensions, the log-transformed distributions are usually flat and follow a straight line, for which the slope is between 2 and 5 (Eisma 1993), but in surface waters and in the nepheloid layer the size distributions are peaked and deviate from the straight line, mostly as a result of biological processes (Stramski et al 1991). This was also the case for Lucinda surface water PSD results (Appendix 4, Figure A11), when power fit was applied to an averaged PSD of all Lucinda samples under the assumption of particles' sphericity (Appendix 4, Figure A13).

Turbidity

During the February 2004 field expedition TSS point sampling was supplemented by in-situ profiling of turbidity measured by an Analite NEP160 turbidity meter provided by Dr Charles Lemckert (Griffith University, Australia). In the instrument submerged into the water sample a beam of light scattered within a broad angle centred on 90˚ is measured by a photomultiplier. The turbidity of the sample is then estimated in nephelometric turbidity units (NTU) relative to standard solutions. Available corresponding turbidity and gravimetric TSS measurements (total 31 pairs) allowed construction of a relationship between the two and thus permitted calibration of the instrument (Figure 3.6). The resulting relationship confirmed the general rule of thumb used by oceanographers, i.e. 1 NTU equals 1 g/m^3 (Ian Jones, personal communication). The turbidity-TSS relationship extended the available pool of TSS data and permitted study of the temporal and depth profiles of flood-mediated suspended sediment concentrations (Chapter 4).

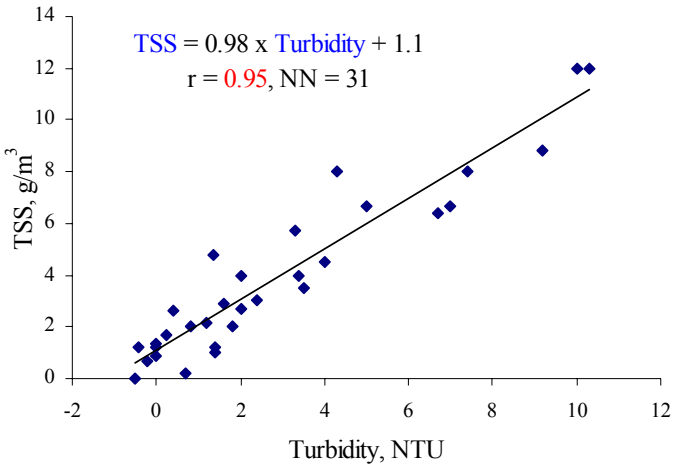

Figure 3.6. Turbidity calibration curve

Visibility

Water visibility is primarily affected by the decrease in irradiance with depth due to scattering and absorbing agents such as suspended solids and coloured dissolved matter. In 1865, the Italian astronomer Pietro Angelo Secchi standardised water visibility estimates by lowering a white disk of about 30 cm diameter into the Mediterranean Sea and measuring the depth at which it became invisible. Although this method is not very accurate, it gives a reliable and quick

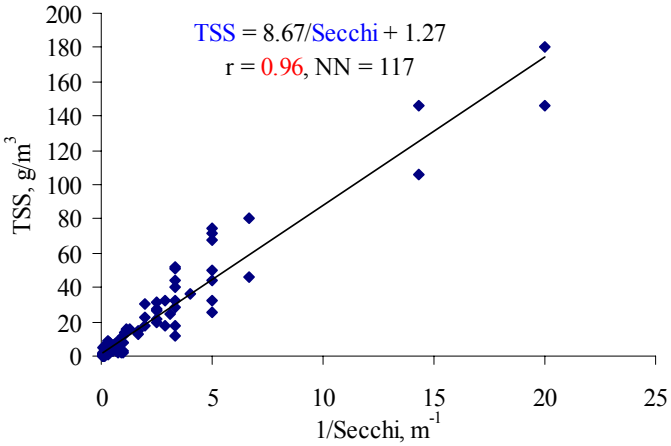

Figure 3.7. TSS-Secchi relationship

estimate of the transparency of the water. During the 2002-2004 Lucinda field trips (except the October 2003 one) Secchi depth measurements were employed to determine the necessary volume of water to be sampled and subsequently filtered. The visibility data as derived from the Secchi disk measurements and corresponding TSS concentrations (total 117 pairs) allowed construction of a TSS-Secchi relationship, which was used to enlarge the TSS dataset in cases where actual in situ measurements were not available (Figure 3.7).

Bottom sediment density

During the October 2003 and February 2004 field expeditions the density of bottom sediments was measured at 23 locations. From each sediment grab a tablespoon (circa 2 cm^3) of sediment was placed into an oven for a minimum of 24 hours at 60ºC. The dried sediment was then added to water of known volume and weight and the new volume and weight were recorded. The sediment density was calculated by the following formula:

$$\text{Density of sediment} = \frac{\Delta V}{\Delta W}, \tag{3.9}$$

where ΔV is the difference between the volume of water with and without sediment, and ΔW is the same but for weight.

Nutrients

The Australian Centre for Tropical and Freshwater Research (James Cook University) carried out determination of nutrient concentrations in water samples collected during February 2004 at Lucinda. Filtration for total filterable nutrients was achieved by pumping the sample directly into 50 mL Terumo polypropylene syringes and then filtering through disposable 0.45 µm Sartorius Mini-Sart cellulose acetate filter modules. In each case the syringes and filters were rinsed several times with sample water prior to collecting the filtrate in the vials.

Samples for total nitrogen, total phosphorus, total filterable nitrogen and total filterable phosphorus were digested using an alkaline persulfate technique (modified from Hosomi (1987)), and the resulting solution was simultaneously analysed for nitrate and FRP by segmented flow autoanalysis using an ALPKEM Flow Solution II (ALPKEM Corporation, Wilsonville, Oregon, U.S.A.). The analyses for NO_X, ammonia and FRP were conducted using standard segmented flow auto-analysis techniques (APHA 1998).

Aerial photography

Aerial photography was carried out on 22 October 2003, and 17 and 20 February 2004. The height of the aeroplane was 2000-3000 feet (equivalent to 610-914 m), which translates into a field of view of about 1 km^2. Aeroplane GPS readings were used to record the positions of reference points (i.e. land, jetty) as well as objects of interest such as plume boundaries. This technique is not particularly precise but it gives an indication of the location of a plume and allows qualitative extrapolation of the plume extent from in situ observations from a boat.

Hydrographic and meteorological data

Hydrographic and meteorological data for the region corresponding to the time of field trips was provided by various agencies. The Department of Natural Resources, Mines and Energy (http://www.nrme.qld.gov.au/) courteously provided data on river heights at Halifax and discharge calculations at Ingham stations, while the Queensland branch of the Bureau of Meteorology (http://www.bom.gov.au/weather/qld/) kindly supplied tide and wind records (both measured at the end of the jetty).

Available satellite imagery

Out of 27 sampling days only five had quality SeaWiFS images: a single image during each of the first three expeditions and two more during February 2004. An effort was made to collect validation data within 40 minutes of direct overpass for coastal stations and within 3 hours for offshore stations, in accordance with the protocols for validation of ocean colour satellite products (Doerffer 2002). In total 24 stations were considered for validation analysis based on temporal and spatial constraints of validation sampling (Figure 3.8).

The acquired SeaWiFS images contained Level-1A High Resolution Picture Transmission (HRPT) data from the Townsville receiving station (TOW), which included raw radiance counts from all bands, spacecraft and instrument telemetry as well as ancillary data (i.e. meteorological and ozone products derived from other agencies). Images were downloaded in Hierarchical Data Format (HDF) ready to be processed by SEADAS (SeaWiFS Data Analysis System), a freely available comprehensive image analysis package for all SeaWiFS data products and ancillary data (http://seadas.gsfc.nasa.gov/).

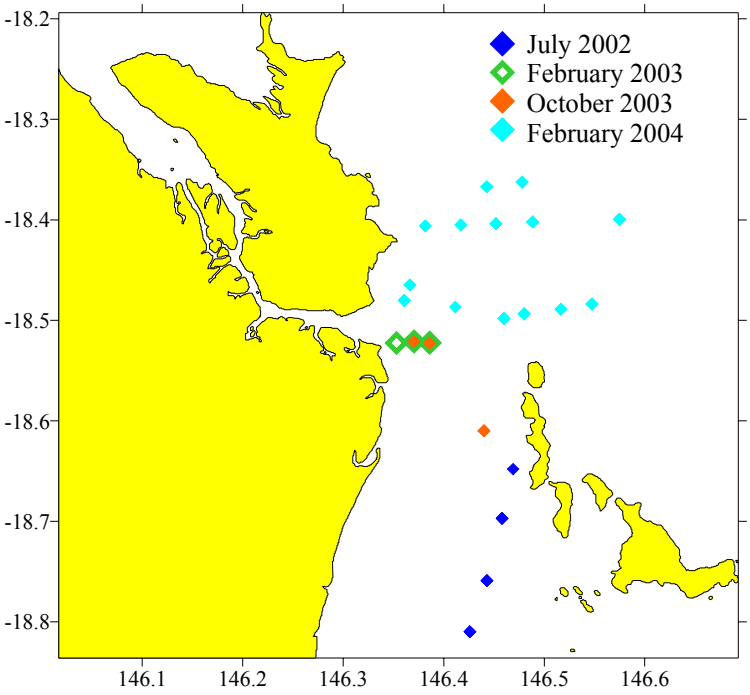

Figure 3.8. SeaWiFS validation stations

Within the objective of validation of the bio-optical model inversion through direct comparisons of in situ and satellite-derived water colouring substances, SeaWiFS validation was the priority for planning and organising field trips. However, starting from the third expedition (October 2003), an effort was made to include in situ measurements coinciding with overpasses of MERIS (MEdium Resolution Image Spectrometer, http://envisat.esa.int/instruments/meris/), an ocean colour sensor on board the European satellite Envisat launched in March 2002, with validated data available starting from July 2003 (ESA 2002). This sensor is designed for both case I and case II waters and as such, its ocean products include biogeochemical water properties such as chlorophyll, total suspended matter and yellow substance concentrations. Therefore, direct comparison between in situ and satellite quantities was possible.

Three cloud-free MERIS images with coinciding in situ measurements were acquired, which resulted in 34 validation stations in October 2003 and February 2004. The higher number of matching stations for MERIS in comparison to SeaWiFS is attributable to the higher spatial resolution of the former (250 m and 1.1 km, respectively).

3.1.3. Implications for remote sensing

In situ measurements overview

All collected and measured data from the 2002-2004 field trips in Lucinda region are graphically presented in Appendix 4. These include station locations (Figure A1), Herbert river discharge for four sampling periods (Figure A2), wind speed for all expeditions except February 2003 (Figure A3), discharges of rivers south of Herbert for the last expedition, February 2004 (Figure A4), tidal climate with corresponding sampling stations (Figure A5), surface chlorophyll concentrations (Figure A6), CDOM absorptions at 440 nm (Figure A7), exponential slopes of CDOM absorption spectra (Figure A8), surface TSS concentrations (Figure A9), organic matter content in TSS (Figure A10), representative PSD (Figure A11), duplicate PSD (Figure A12), Junge slopes calculated for various size ranges (Figure A13), and bottom sediment densities (Figure A14).

The following or a combination of the following sources govern variability of biogeochemical and optical parameters in coastal ocean at Lucinda:

1. *Proximity to the shore*. The effect of the seashore on coastal water properties can be twofold. On the one hand, the presence of a river entering the coastal ocean translates into proximity of a strong nutrient and sediment source. On the other hand, in shallow waters subject to tides or wind resuspension, an onshore gradient of turbidity is expected. For Lucinda data the combination of both factors is well illustrated by East-West and West-East transects north and south of the jetty in February 2004 (C20.J1-C20.J10), where the three substances of interest exhibited clear decreasing offshore and increasing onshore gradients (Figures A6, A7, A7).
2. *River flood and associated plumes.* River flood effect on water properties is evidenced by February 2004 time series of TSS and nutrients at the Herbert River mouth (station Mariner). This is discussed in more detail in the following chapter. Resultant plumes of the quantities of interest were observed during and after the moderate flood in February 2004 and are described in the last part of this section.
3. *Seasonality.* Variability between seasons is particularly pronounced through comparison of July 2002 and February 2004 offshore stations where average TSS, CHL and CDOM for dry-season July 2002 (0.82 g/m^3, 0.22 mg/m^3, 0.12 m^{-1}, respectively) were 2-4 times smaller than those for wet-season February 2004 (2.48 g/m^3, 0.77 mg/m^3, 0.23 m^{-1}, respectively).
4. *Tidal phase.* Tidal effect on distributions of water properties is relevant in tidally affected areas, i.e. deltas. February 2004 time series of TSS and nutrients at Mariner

station before and after the flood evidence the importance of the tidal phase factor, which is further discussed in the following chapter.

5. *Biological fronts.* There are four prerequisites for phytoplankton growth: energy in the form of solar radiation, inorganic carbon in the form of CO_2 or bicarbonate ions, mineral nutrients, and water. Of those, the first and the third can be limited in natural marine environments. In the open ocean there is usually plenty of light but no nutrients, but in estuaries and shallow zones the opposite is true: while most of the nutrients are supplied by rivers or nutrient-rich sediment resuspension, turbidity associated with suspended particles produces light deficiency. Consequently, highly productive zones usually occur some distance off river mouths where nutrients would had arrived with river plumes and turbidity would have become low enough to allow sufficient light for phytoplankton growth, due to gravitational settling of suspended matter. Such a scenario and an associated phytoplankton bloom (possibly Trichodesmium although in the late stage of development) were observed during the last field expedition about 20 km to the northeast of the Herbert River mouth.

Optical type of waters at Lucinda

Case I waters are defined as waters for which phytoplankton and their associated and co-varying materials (such as excreted particulate and dissolved organic matter) control the optical properties (Gordon et al 1983). To the extent that the quantification of these materials (living and inanimate) is operationally made through the determination of a single pigment, i.e. chlorophyll_*a*, it can be said that the optical properties of such waters depend only on CHL concentration. In contrast, in case II waters there are three independent water-colouring components, notably TSS, CHL and CDOM. Therefore, differentiation between the two cases lies not in the magnitude of concentrations of water-colouring constituents (in fact, case I waters can range from oligotrophic or phytoplankton-poor to eutrophic or phytoplankton-rich) but rather in mutual relationships among the three constituents.

For ocean colour-related research in coastal waters, knowledge of optical type of the waters studied is desired. To address this issue, the nature of the relationships among the major optically significant substances must be established. For such analysis in Lucinda waters, all stations were categorised as coastal ocean or open ocean. A station was classified as belonging to an open ocean group if it was located more than 10 km offshore from the Hinchinbrook Channel entrance. The coastal ocean group included the first half of the jetty, the channel and river stations. Stations located in areas periodically affected by tides and river plumes (waters beyond mid-jetty and less than 10 km off the channel entrance) were excluded

from the present analysis as they could exhibit characteristics of both groups; hence their inclusion in either one would be subjective. It should be noted that the above classification refers to the region of study and may be different if a larger area (e.g. waters outside the GBR lagoon) is considered.

Relationships between major optically significant substances can be expressed in terms of the statistical significance of associations between variables. In the simplest mode this can be tested by means of Pearson's correlation coefficient. Results of cross-correlation analysis for six biogeochemical and optical properties measured in Lucinda waters during four field expeditions are presented in Table 3.2 with statistically significant values at 95 %, 99 % and 99.9 % highlighted. Correlation coefficients as well as their statistical significance levels were calculated for all data as well as for the open ocean and coastal ocean subsets.

CDOM	**0.59** (69) **0.70** (19) **0.59** (42)				
TSS	**0.31** (125) **0.47** (36) 0.13 (61)	**0.27** (70) 0.25 (19) 0.21 (41)			
OSS	0.28 (33) 0.17 (10) 0.06 (19)	**0.50** (28) 0.51 (6) 0.45 (18)	**0.95** (38) **0.87** (12) **0.96** (22)		
OSS/TSS	**-0.76** (33) -0.52 (8) **-0.73** (19)	-0.28 (28) -0.75 (6) 0.17 (18)	**-0.51** (38?) -0.38 (12) **-0.51** (22)	**-0.43** (38) 0.08 (12) -0.40 (22)	
S_{CDOM}	-0.05 (68) 0.36 (19) -0.19 (42)	-0.06 (70) 0.05 (19) -0.10 (44)	0.14 (70) 0.07 (19) 0.26 (43)	-0.05 (28) -0.60 (6) 0.25 (18)	0.07 (28) -0.33 (6) 0.31 (18)
	CHL	**CDOM**	**TSS**	**OSS**	**OSS/TSS**

Table 3.2. Correlations between measured biogeochemical and bio-optical properties in the Lucinda waters. Number of correlated stations is shown in brackets. Correlation significant at < 0.001 is shown in red, < 0.01 in green, and < 0.05 in blue. The top line is for all stations, the middle for the open ocean group, and the bottom for coastal stations.

The major findings from this correlation analysis can be summarised as follows:

- CDOM is significantly correlated with CHL, with a particularly tight relationship for the open ocean stations. Therefore, phytoplankton seems to act as both a source and a sink of CDOM for these waters, the latter through consumption of remineralised organic matter and the former through excretion after the death of phytoplankton.
- TSS is significantly correlated with CHL in the open ocean waters, while no association was found for coastal stations. The open ocean correlation is strong enough to affect the all stations relationship; as a result, the correlation between TSS

and CHL is statistically significant for all stations. Organic suspended matter, on the other hand, is not significantly correlated with CHL for any combination of stations.

- TSS is weakly but significantly (at 95 %) correlated with CDOM for all available stations. Smaller insignificant correlation coefficients were found for both open ocean and coastal ocean stations, suggesting that proximity to the shore and hence offshore decreasing trends in both substances are behind the all-stations relationship.
- The correlation of organic suspended sediment OSS with CDOM in Lucinda waters exhibits similar behaviour although with about 2-fold stronger correlations for all station combinations. Considering this and the previous finding it can be concluded that the correlation of TSS with CDOM is attributable to organic fraction in sediments – a reasonable assumption as part of CDOM is the product of microbial reworking of OSS.
- TSS is negatively correlated with the organic matter content in TSS in coastal ocean waters, which is reflected in the all-stations significant correlation coefficient. Such associations can be related to (i) the general inverse correlation between organic matter content and suspended matter concentration found in rivers (Eisma 1993), (ii) resuspension-affected surface concentrations of TSS, as bottom sediments in the Herbert River and adjacent coastal waters have low organic content (Charles Lemckert, personal communication), and (iii) the fact that biogenic particles comprise the bulk of the suspended material in the surface waters of the open ocean (Eisma 1993).
- Little or no correlation was found between the exponential slope of CDOM and other analysed biogeochemical and optical properties. The independent behaviour of this optical parameter is controlled by factors unrelated to common sources of variability defined in the previous section. These factors, which affect the spectral dependence of dissolved matter, include photodegradation, chemical transformations due to changing salinity, flocculation and precipitation at low salinities, atmospheric deposition, and diffusion from bottom sediments (Hansell et al 2002).

Overall, the studied waters beyond the influence of the Herbert River fall under the definition of case I waters, with both CDOM and TSS tightly coupled with chlorophyll. On the other hand, coastal waters at Lucinda can be classified as intermediate between case I and case II types, as one of the water-colouring constituents, CDOM, is related to CHL while TSS is independent of both CDOM and CHL.

Optical significance of water-colouring constituents at Lucinda

For optically complex natural waters it is useful to have a single term to characterise their optical properties. Throughout the history of ocean optics science, various classification schemes have been introduced. Initially they were based on various optically-related criteria such as transmittance of downward irradiance (Jerlov 1976) and vertical attenuation coefficient (Pelevin et al 1977), while somewhat more biogeochemically-oriented schemes assessed the relative contributions of water-colouring constituents to inherent optical properties of waters (Kirk 1994; Sathyendranath 2000). The now classical separation into case I and case II waters, first introduced by Morel and Prieur (1977), can be considered a simplified case of the optical classification scheme subsequently proposed by Prieur and Sathyendranah (1981). The idea is to take an optical property of interest (say, absorption coefficient) at a certain wavelength and compute partial contributions to this property from major water-colouring substances, namely, CHL, CDOM and TSS. The resultant three-dimensional point can then be plotted on a triangular diagram in which the sides of the triangle represent the fractional contributions attributable to each of the components. The relative position of a point on the diagram would give an indication of the relative importance of these substances in the water optical signal.

The approach described above was applied to the Lucinda stations, which had simultaneous measurements of all three substances. The inherent optical property chosen was absorption coefficient, which was calculated for each of the triplets of water-colouring constituents by the forward bio-optical model with the average optical parameters (Table 2.1, section 2.2). Results for total of 68 stations are presented in Figure 3.9a-c for three wavelengths at which cumulative absorption (i.e. total absorption minus water absorption) is most affected by one of the optical substances: 412 nm (CDOM), 443 nm (CHL) and 555 nm (TSS). The stations are separated into coastal ocean and open ocean subsets according to the criteria set above. Also a diagram highlighting different field expeditions is presented (Figure 3.9d), which provides an idea of the importance of seasonality in the regional optical properties.

Because the majority of the points on the diagrams tend to cluster along the TSS-CDOM axis, Lucinda waters can be classified as CDOM- and TSS-dominated waters, with a slight tendency of open ocean to be more CDOM-dominated and coastal ocean more TSS-dominated. The contribution of CHL and hence phytoplankton to cumulative absorption is below 20 % at all wavelengths studied, which is actually less for total absorption coefficient as water absorption is not included in the current estimates. The only station, which had circa 50 % contribution of CHL absorption to the optical signal at 443 nm, was the most offshore

station, near Bramble Reef (Febr04_C20.6). Therefore, only two water-colouring components can be considered optically significant in Lucinda waters – dissolved and particulate non-chlorophyllous matter.

The above-mentioned tendency of coastal waters to be more optically TSS-dominated is probably due to (i) the extra sediment source arising from resuspension in shallow waters and (ii) the larger inorganic content in the sediments closer to the shore (as evident from the correlation analysis above) and thus much stronger backscattering signal of these sediments.

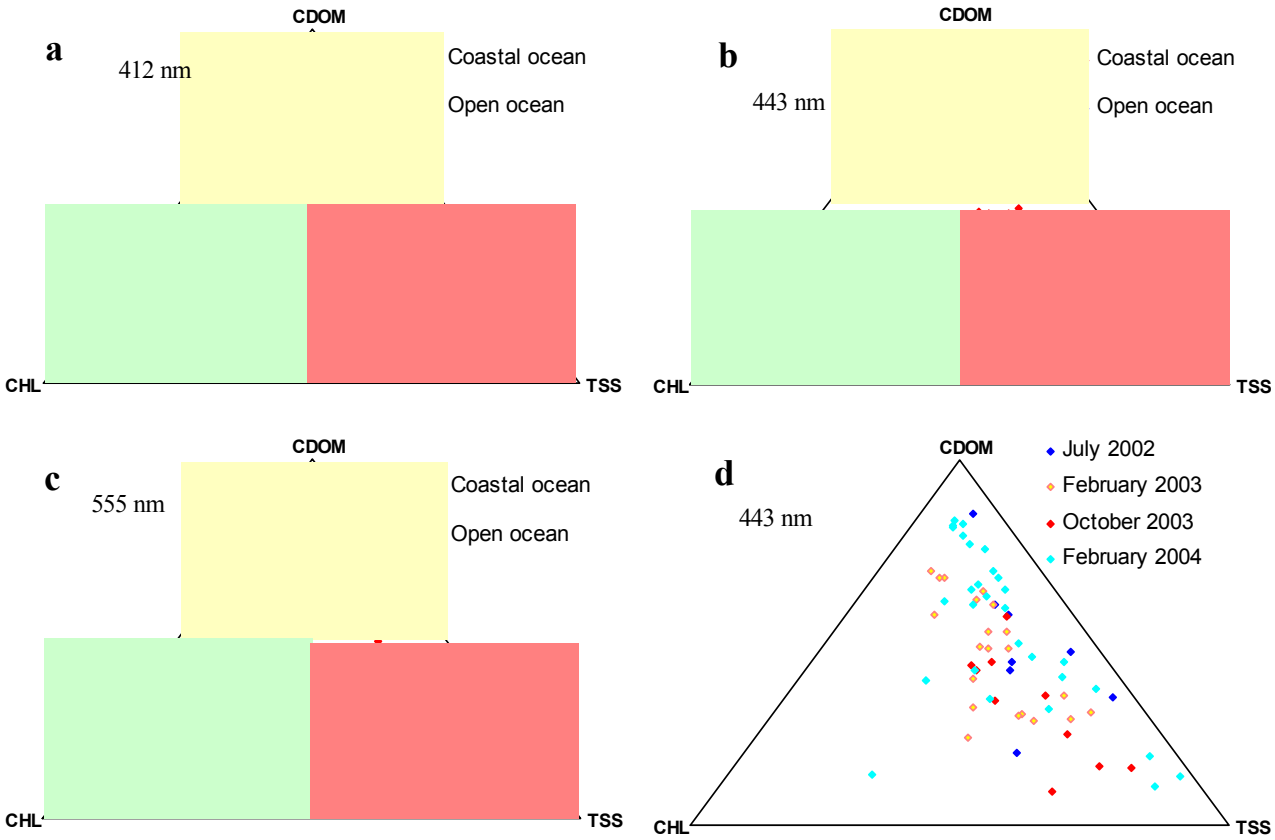

Figure 3.9. Relative contribution of water-colouring constituents to cumulative absorption coefficient at 412 nm (a), 443 nm (b), 555 nm (c) for coastal and open-ocean stations (a-c) as well as for various field expeditions at 443 nm (d). Shaded areas correspond to optical dominance of CDOM (yellow), TSS (red) and CHL (green).

Separation of the data according to the field expeditions and hence various seasons did not result in clustering of stations based on this criterion. Slight biases towards CDOM in February 2003 and TSS in October 2003 are probably related to sampling locations (more river stations in February) rather than to actual differences in water properties. Overall, in the context of optical significance of water-colouring components, Lucinda waters can be considered temporally homogeneous with without pronounced seasonality. At the same time,

as mentioned earlier in this section, the substances examined exhibit clear seasonal trends in terms of absolute values. Combining the above considerations, TSS and CDOM, for example, can exhibit lower concentrations during a dry season in comparison to a wet period, but their relative optical contributions to cumulative absorption are likely to be the same for both seasons. This example indicates that while concentrations of water-colouring constituents can change due to the sources of variability outlined, the optical type of the studied waters can be considered invariant for the region.

Aerial mapping of plumes

Aerial surveillance is often used to define the geographical limits of riverine plumes entering the GBR lagoon, and in some instances to monitor the movement of a plume over a period of time (Devlin et al 2001). On 17 February 2004, 5 days after the peak of the moderate flood in the Herbert River, concurrent measurements of in situ properties were supplemented by GPS positioning of plume crossings from an aeroplane as well as by aerial photography. Resultant distributions of parameters with locations of the boundaries of observed plumes as recorded remotely from the air are shown in Figure 3.10.

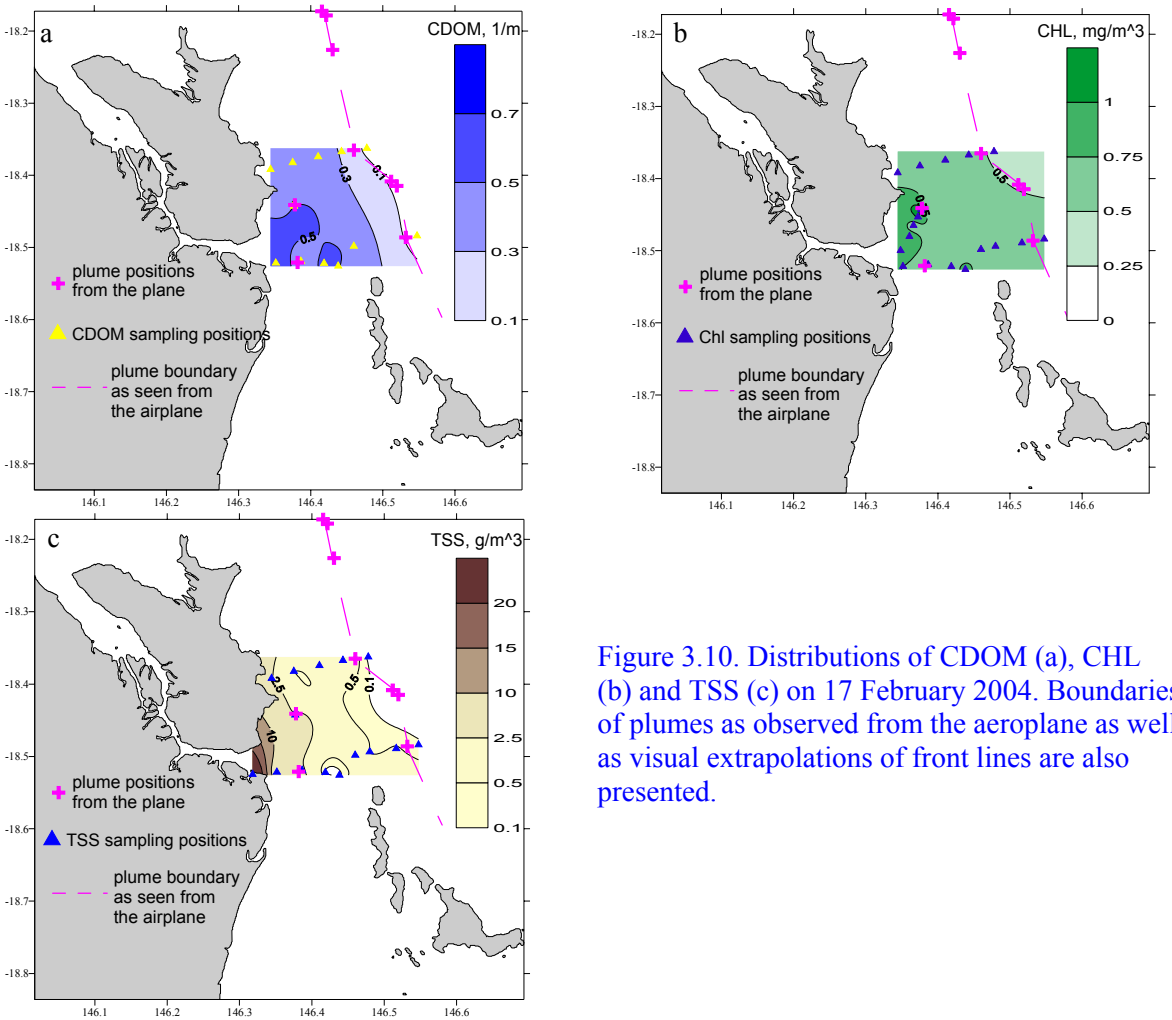

Figure 3.10. Distributions of CDOM (a), CHL (b) and TSS (c) on 17 February 2004. Boundaries of plumes as observed from the aeroplane as well as visual extrapolations of front lines are also presented.

The extent of the offshore plume was readily observable from the plane, with a sharp edge and a slight colour change within and outside the plume (Figure 3.11a). The front line was located halfway between the mainland and Bramble Reef, and as the furthest detected extent of the floodwaters is the primary candidate to reach and possibly affect the mid-shelf coral reefs. In terms of parameter concentrations, the plume was bounded by the 0.1 m^{-1} isoline of CDOM absorption, approximately 0.5 mg/m^3 of CHL concentration and between 0.01 and 0.5 g/m^3 of TSS concentration.

Figure 3.11. Offshore (a) and coastal (b) plumes on 17 February 2004 as observed from the aeroplane

The front as observed from the plane coincided best with the distribution of dissolved organics. Indeed, applying the forward bio-optical model and estimate contributions of each of the water-colouring constituents to the total absorption coefficient (which is much greater than the backscattering term and thus determines the water-leaving optical signal), it can be readily seen that CDOM absorption dominates contributions from other terms throughout the visible spectrum (Figure 3.12).

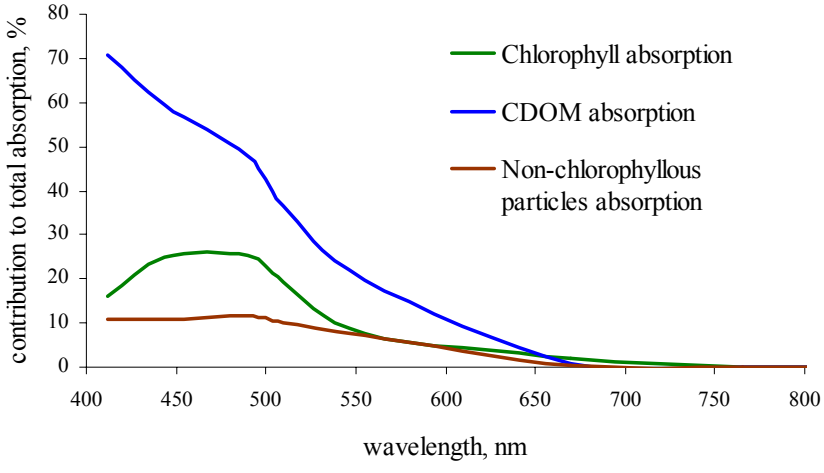

Figure 3.12. Relative contribution of water-colouring constituents to total absorption coefficient at the edge of the offshore plume on 17 February 2004.

It is worth noting that concentrations of all the biogeochemical quantities studied on either side of the offshore plume are low, with very small gradients across the boundary. Consequently, the plume edge is subject to disappearance under favourable conditions such as wind mixing. This assertion is also supported by CTD-derived salinity and temperature profiles across the plume (Mal Heron, unpublished data). Such a scenario must indeed have occurred, as aerial photographic images taken 3 days later, on 20 February 2004, did not show any visible plumes at similar or further offshore locations.

The coastal plume, on the other hand, was characterised by a sharp boundary highlighted by a foam line and a dramatic colour change from brown turbid water masses to contrasting cleaner waters outside the plume (Figure 3.11b). The front line matched the measured TSS distribution best, although application of the absorption contribution technique to this plume revealed that it was CDOM that dominated the optical plume extent. The reason for such a discrepancy lies in the fact that the time difference between boat sampling and aeroplane survey of the coastal plume was about one hour. The offshore plume sampling, on the other hand, coincided with the direct aeroplane overpass. Therefore, considering the highly dynamic tidally driven nature of the coastal plume, the positions as recorded from the aeroplane might not correspond to the distributions of measured quantities.

In conclusion, CDOM appears to play a significant role in colouring the coastal waters at Lucinda and to define ocean colour of both fresh tidal and residual flood plumes. The latter, although readily observable from the air, is characterised by low concentrations and minor across-boundary gradients of optically significant substances. Therefore, when interpreting aerial photography for the purposes of plume mapping, it should be kept in mind that such plumes (i) are not stable formations and therefore have little chance of reaching mid-shelf coral reefs; and (ii) are characterised by concentrations which are hardly different from the ambient values in reef ecosystems.